

## Electronic Supplementary Information for

# A monocarboxylic acid induction strategy to prepare tough and thermos-reversible poly(vinyl alcohol) physical gels with high transparency

Weifeng Zhong, Yufang Song, Shuai Yang, Lihao Gong, Dongjian Shi, Weifu Dong  
and Hongji Zhang\*

The Key Laboratory of Synthetic and Biological Colloids, Ministry of Education, School of Chemical and Material Engineering, Jiangnan University, Wuxi, Jiangsu 214122, China.

\* Corresponding author: Prof. Hongji Zhang

E-mail: [hongjizhang@jiangnan.edu.cn](mailto:hongjizhang@jiangnan.edu.cn)

## This PDF file includes:

Experimental Section

Table S1 to S2

Fig. S1 to S12

## EXPERIMENTAL SECTION

### Materials

Poly(vinyl alcohol) (PVA 1799, 98%~99% hydrolyzed, Mw 73000-78000), dimethyl sulfoxide (DMSO, 99%, analytical reagent), propionic acid (PA, 99.5%, analytical reagent), butyric acid (BA, 99.5%, analytical reagent), DL-malic acid (DMA, 99%, analytical reagent) and citric acid (CA, 99.5%, analytical reagent) were purchased from Aldrich Biochemical Technology Co., Ltd (Shanghai, China). Hydrochloric acid (HCl, 36.5%-38 wt%), formic acid (FA, 98%, analytical reagent), and acetic acid (AA, 99.5%, analytical reagent) were obtained from Sinopharm Chemical Reagent Co., Ltd. (Shanghai, China). Glutaraldehyde (25 v%) was obtained from Macklin Biochemical Technology Co., Ltd. (Shanghai, China). All the above materials were used as received without further purification. Deionized water was provided by Jiangnan University.

### Methods

**Preparation of PVA physical gels.** Different small molecules of carboxylic acids (formic acid, acetic acid, propionic acid, butyric acid, DL-malic acid, citric acid) were added to 20 mL of dimethyl sulfoxide (DMSO) to form different concentrations of carboxylic acid DMSO solutions. 5 g of PVA was dissolved in the above solution at 95 °C with the assistance of mechanical agitation for 3 h, making the concentration of PVA 25 w/v%. After sufficient defoaming, the homogeneous solutions were transferred to molds (two 10 cm × 10 cm glass plates separated with a 2 mm silicone spacer) and then the PVA physical gel was obtained after 12 h of standing at room temperature. The as-prepared gels were denoted as PVA/D-Xy, in which X represented the carboxylic acids and y for their concentration.

For the PVA physical gels induced at different times, the gels were prepared by 3 mol·L<sup>-1</sup> acetic acid DMSO solution and standing at room temperature for different times through the aforementioned method. The as-prepared gels were denoted as PVA/D-AA3-a, in which a represented the induction time.

**Preparation of PVA hydrogels.** The PVA hydrogels were prepared by soaking the aforementioned PVA physical gels in deionized water for 24 h by exchanging water every 8 h. The as-prepared hydrogels were denoted as PVA/W-Xy.

**Preparation of PVA aqueous solution containing 2 M acetic acid.** The acetic acid was dissolved in 20 ml DI water to form a 2 mol/L AA aqueous solution. 5 g of PVA was dissolved in the above AA solution at 95 °C with the assistance of mechanical agitation for 3 h, making the concentration of PVA 25 w/v%. After sufficient defoaming, a portion of the homogeneous solutions was transferred to a vial and kept at room temperature for 12 h, 36 h, and 72 h to observe the state changes.

### Characterizations

Fourier transform infrared spectroscopy (FT-IR) of PVA 1799, PVA physical gels, and the lyophilized PVA hydrogels were carried out using a Nicolet iS50 instrument (Thermo Fisher Scientific, USA) with attenuated total reflectance (ATR) in the wavenumber range of 650 to

4000 cm<sup>-1</sup> with 32 scans and a nominal resolution of 4 cm<sup>-1</sup>. A field emission scanning electron microscope (FE-SEM, Hitachi S-4800, Japan) was used to observe the morphologies of the samples. Prior to SEM analysis, the as-prepared physical gels were immersed in deionized water for 24 h to convert DMSO to water, and then the gels were cryogenically quenched under liquid nitrogen and freeze-dried to reveal their internal cross-sectional structure. The surface of the samples was sputter-coated with gold to create a conductive environment.

**Differential scanning calorimetry (DSC) measurements.** The crystallinities of the PVA physical gels and PVA hydrogels were measured by a differential scanning calorimeter (DSC 204 F1, NETZSCH-Gerätebau GmbH, Germany). Before DSC measurements, the PVA physical gels were first excess chemical crosslinked by soaking in an aqueous solution composed of glutaraldehyde, hydrochloric acid, and deionized water (volume ratio = 20:1:50) for 2 h to fix the amorphous PVA polymer chains and convert DMSO to water, minimizing the formation of further crystalline domains during the freeze-drying process.<sup>1</sup> Subsequently, the samples were immersed in a large amount of DI water for 12 h to get rid of the residual glutaraldehyde, hydrochloric acid, and other small molecules. Following lyophilization, the dry samples were heated up from 50 to 250 °C at a scanning rate of 20 °C min<sup>-1</sup> under a nitrogen flow of 30 ml min<sup>-1</sup>. The broad peak from 60 to 180 °C and the narrow peak from 200 to 250 °C on the curve of heat flow respectively correspond to the evaporation of the residual water and the melting of the PVA crystalline domains. Calculate the integration of the endothermic enthalpy of two regions, expressed as  $H_w$  and  $H_c$ , respectively. Consequently, the crystallinity of the samples  $X_c$  can be calculated using the following equation:

$$X_c = (H_c \times H_w^0) / [H_c^0 \times (H_w^0 - H_w)]$$

Where  $H_c^0 = 138.6 \text{ J g}^{-1}$  is the enthalpy of the fusion of 100 wt% crystalline PVA measured at equilibrium melting point,  $T_m^0$ ,<sup>2</sup> and  $H_w^0 = 2260 \text{ J g}^{-1}$  is the latent heat of water evaporation.<sup>3</sup>

**X-ray diffraction measurements.** X-ray diffraction (XRD) was recorded on a Bruker D8 diffractometer (German Bruker AXS, Germany) using Cu K $\alpha$  radiation with the 2 $\theta$  range from 10 to 60° at a scanning rate of 4° min<sup>-1</sup>. Before XRD measurements, the samples underwent the same treatment as for DSC measurements.

**Water content measurements.** The water content (WC) of the PVA hydrogels was measured by comparing their weights before and after drying. We first weighed the weight of the PVA hydrogels after the extra surface water had been wiped off and represented it as  $m_w$ . The PVA hydrogels were then dried in a vacuum oven at 60 °C for 3 days till totally dried and the weight was noted as  $m_d$ . The water content was calculated as follows:  $WC = [(m_w - m_d)/m_w] \times 100\%$ .

**Mechanical measurements.** The mechanical properties of the PVA physical gels and PVA hydrogels were performed with a universal double-column bench testing machine (5967X, ITW Company, USA) at room temperature. For the tensile experiment, the samples were cut into dumbbell-shaped pieces (gauge length: 17 mm; inner width: 4 mm; thickness: 2 mm) and stretched at a crosshead speed of 50 mm min<sup>-1</sup>. The tensile strain was estimated as the change in length relative to the initial length, and the stress was obtained by dividing the force with the initial cross-sectional area of the sample. Elastic modulus  $E$  was calculated from the linear region slope of the stress-strain curve, while toughness was defined as the area under the stress-strain curve until the sample cracked. For the loading-unloading tests, the sample was stretched to a certain strain (200%) and unloaded at 50 mm min<sup>-1</sup>. The dissipated energy was

evaluated from the closed area of the hysteresis loop between the loading-unloading curve.

**Rheological properties.** The viscoelasticity of the PVA physical gels and PVA hydrogels was evaluated at 25°C using a DHR-3 rheometer (TA Instruments, USA) in oscillation mode. Before the frequency sweep, the dynamic strain sweep was measured and the strain was determined to be 0.1% to ensure that the rheological measurements were within a linear viscoelastic range. Then the samples were put between the parallel plate (20 mm in diameter) with an angular frequency from 0.1 to 100 rad s<sup>-1</sup> at a constant strain of 0.1%. The temperature sweep was measured from 25 to 90 °C (5 °C min<sup>-1</sup>) at a constant angular frequency of 10 rad s<sup>-1</sup> and a strain of 0.1%.

**Transparency measurements.** The transmittance of PVA physical gels and PVA hydrogels up to 2 mm thick were assessed on a UV-3600iPLUS spectrophotometer (Shimadzu Corporation, Japan) in the wavelength range from 400 to 800 nm with a resolution of 0.5 nm.

**Table S1. The gelation time of PVA physical gels with 2 mol L<sup>-1</sup> different small molecular monocarboxylic acids.**

PVA concentration (w/v%)	Small molecular monocarboxylic acid	Small molecular concentration (mol L <sup>-1</sup> )	Gelation time (min)
25	formic acid (FA)	2	50
25	acetic acid (AA)	2	34
25	propionic acid (PA)	2	26
25	butyric acid (BA)	2	15

**Table S2. The gelation time of PVA physical gels with different acetic acid concentrations.**

PVA concentration (w/v%)	Small molecular monocarboxylic acid	Small molecular concentration (mol L <sup>-1</sup> )	Gelation time (min)
25	acetic acid (AA)	1.5	120
25	acetic acid (AA)	2	34
25	acetic acid (AA)	2.5	18
25	acetic acid (AA)	3	8
25	acetic acid (AA)	4	2



**Fig.S1** Digital images of different times after 2 M acetic acid was introduced into PVA aqueous solution.

As shown in Fig. S1, when the solvent was changed to water, gelation could not occur and remained in a flowing state at 12h, 36h, and 72h, no trend of gelation was found. This indicates that the monocarboxylic acid induction strategy is not applicable in the PVA/ H<sub>2</sub>O system, which may involve the allocation of hydrogen bond sites. H<sub>2</sub>O can serve as both a hydrogen bond acceptor and a hydrogen bond donor. When monocarboxylic acid is introduced into the PVA/ H<sub>2</sub>O system, a complex hydrogen bonding system will be formed, and no or only very few parts of the intra/inter-chain hydrogen bonds of PVA chains can be restored, which is not enough for gelation.

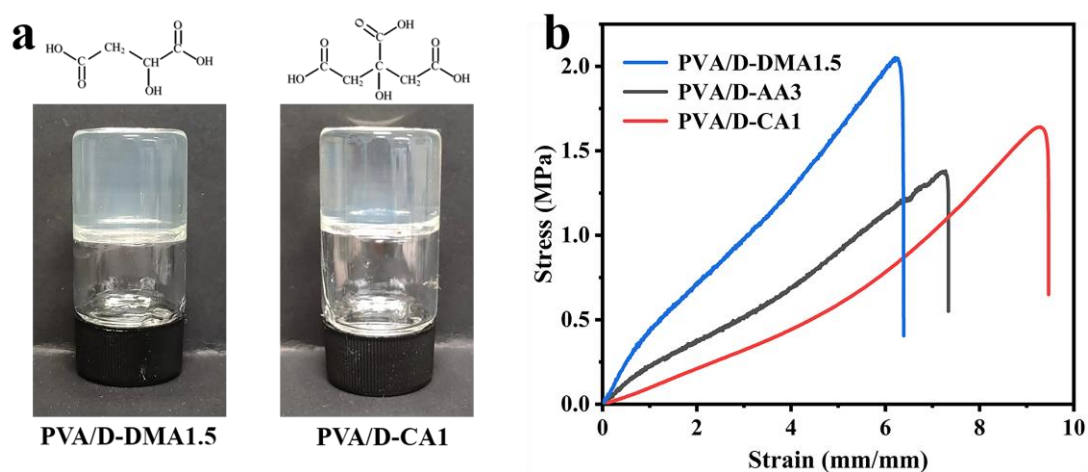


**Fig. S2** (a) Digital images of PVA physical gels induced by 1.5 M DL-malic acid and 1 M citric acid. (b) Tensile stress-strain curves of PVA/D-AA3, PVA/D-DMA1.5, and PVA/D-CA1.

Two polycarboxylic acids, dicarboxylic DL-malic acid (DMA), and tricarboxylic citric acid (CA) were selected to verify whether polycarboxylic acids can induce the PVA/DMSO system into gels. According to Fig. S2a, DMA and CA could induce the gelation of the PVA/DMSO system. We further explored the effects of different carboxylic acids at the same carboxylic group concentration (3 M) on the mechanical properties of PVA physical gels as depicted in Figure

S2b. Under the same carboxyl group concentration (3 M), PVA physical gel induced by DMA had higher tensile strength but lower elongation at break than that induced by AA, whereas PVA physical gel induced by CA had both higher tensile strength and elongation at break than that induced by AA. The relationship between the structure of polycarboxylic acids and the characteristics of induced PVA physical gels needs to be further explored.

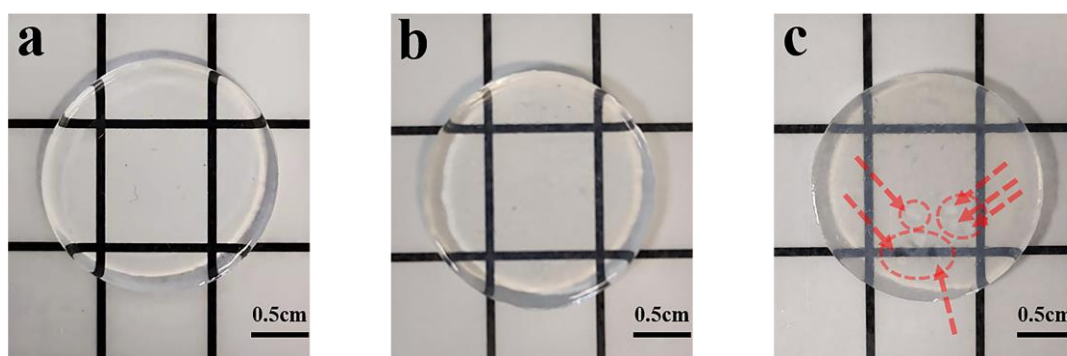


**Fig. S3** Digital images of (a) PVA/D-AA2, (b) PVA/D-AA3, and (c) PVA/D-AA4 gel.

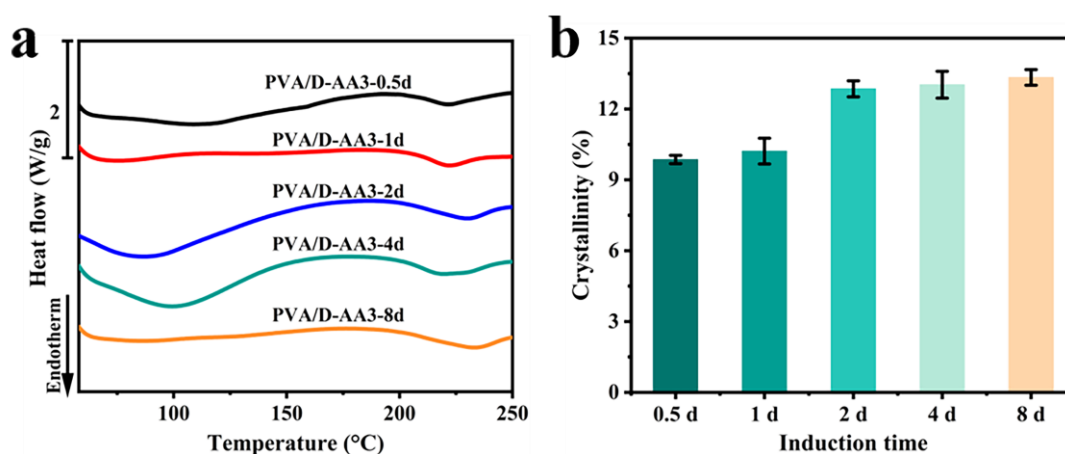


**Fig. S4** (a) Representative DSC thermographs and (b) Crystallinity ( $X_c$ ) of PVA/D-AA3 gels with different induction times.

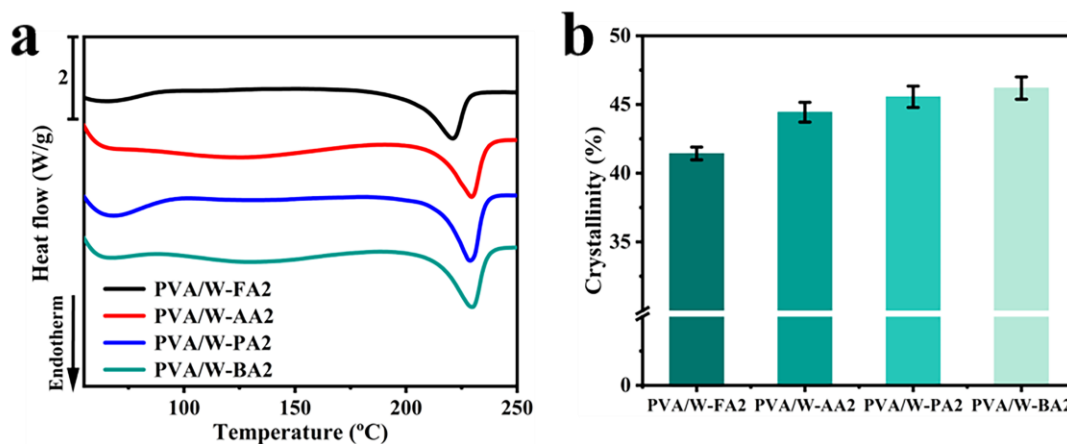


**Fig. S5** (a) Representative DSC thermographs of the PVA hydrogels induced by 2 M different monocarboxylic acids. (b) Crystallinity ( $X_c$ ) of the PVA hydrogels induced by 2 M different monocarboxylic acids.

The DSC curves and crystallinity of PVA hydrogels (at a dry state) obtained through the soaking strategy were depicted in Fig. S5, compared to PVA physical gels, the crystallinity of PVA hydrogels was significantly improved, reaching approximately four times that of corresponding PVA physical gels. This is explained by the hydrophobic interaction between PVA chains during the solvent exchange process, which promotes the orderly aggregation of PVA chains to form crystallization regions.<sup>4,5</sup>

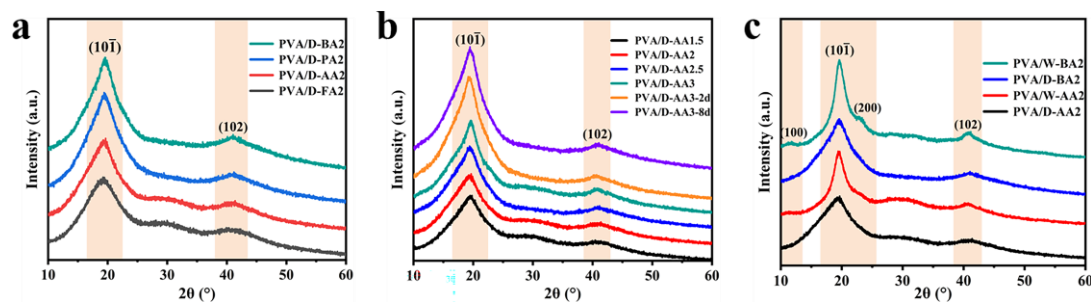


**Fig. S6** XRD patterns of (a) PVA/D-AA gels induced by 2 M different monocarboxylic acids, (b) PVA/D-AA gels induced by different AA concentrations, and PVA/D-AA3-2d gel and PVA/D-AA3-8d gel, and (c) PVA physical gels and hydrogels induced by 2 M acetic acid and butyric acid.

All the XRD curves exhibited two diffraction peaks at  $2\theta = 19.4^\circ$  and  $2\theta = 40.8^\circ$ , corresponding to the typical defined (101) and (102) planes of PVA crystallites, respectively. With the growth of the alkyl chain of the monocarboxylic acid, the peaks of (101) and (102) planes became sharper and their intensities increased obviously (Fig. S6a). In addition, when the AA concentration and induction time increased, the peaks of (101) and (102) planes also became sharper and more intense, and their intensities stabilized after induction for more than two days (Fig. S6b). It was worth noting that the PVA hydrogels presented sharper and

larger peaks at  $2\theta = 19.4^\circ$  and  $2\theta = 40.8^\circ$  compared to the corresponding PVA physical gels before immersion, and PVA/W-BA2 revealed new diffraction peaks at  $2\theta = 12.2^\circ$  and  $2\theta = 22.5^\circ$ , corresponding to the lattice planes of (100) and (200) (Fig. S6c).

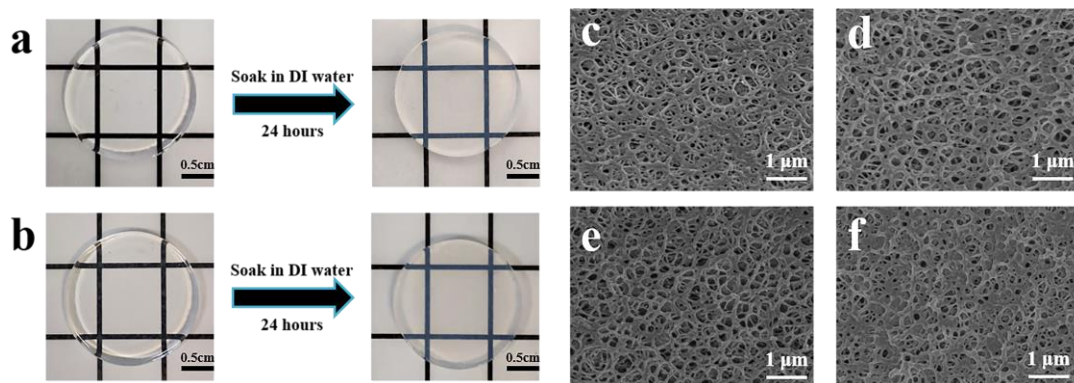


**Fig. S7** Digital images of (a) PVA/D-AA2 and PVA/W-AA2, (b) PVA/D-BA2 and PVA/W-BA2. SEM images of (c) PVA/W-FA2, (d) PVA/W-AA2, (e) PVA/W-PA2, and (f) PVA/W-BA2 hydrogels.

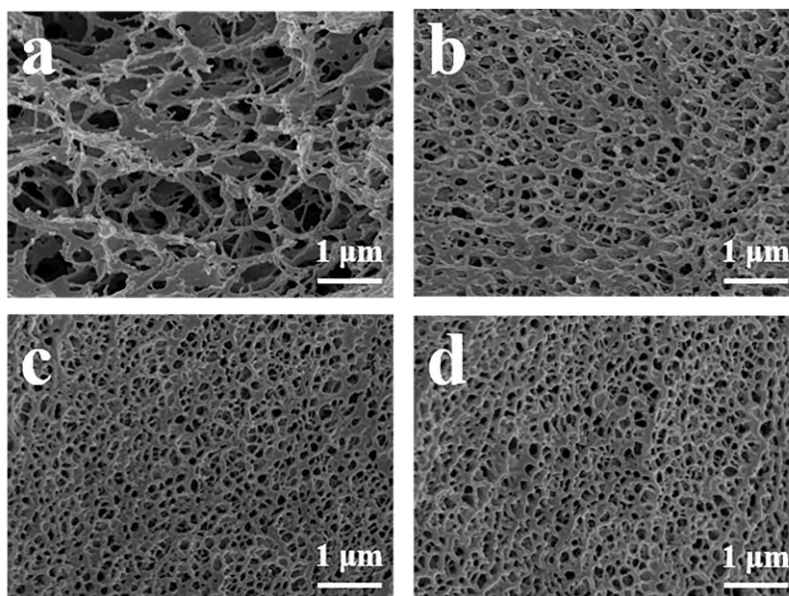


**Fig. S8** SEM images of (a) PVA/W-AA1.5, (b) PVA/W-AA3, (c) PVA/W-AA3-2d, and (d) PVA/W-AA3-8d hydrogels.

Since the PVA physical gels with DMSO as the solvent cannot be frozen using the traditional lyophilization method, we immersed the PVA physical gels in DI water for 24 h to obtain PVA hydrogels. As shown in Fig. S7a and b, the volume of the gels barely changed after 24 h of immersion, the PVA hydrogels obtained from solvent exchange had anti-swelling capacity<sup>6</sup>

so it could be assumed that the solvent exchange strategy does not change the skeleton structure of the gels and the morphology of PVA hydrogels could reflect the morphology of PVA physical gels. The micromorphology of PVA hydrogels revealed a three-dimensional porous structure, which could be efficient in dissipating applied force to strengthen mechanical properties. The average pore size of PVA/W-FA2 was roughly 530 nm, while PVA/W-AA2, PVA/W-PA2, and PVA/W-BA2 hydrogels presented smaller pore sizes of 420 nm, 360 nm, and 240 nm (Fig. S7c-f), resulting from the enhanced intermolecular interaction and increased cross-linking density. The water content measures of PVA hydrogels also proved consistent results (Fig. S9). Subsequently, we analyzed the variation of micromorphology with the enhanced AA concentration and induction time. With an increase in AA concentration, the networks on the fractured surfaces became more compact, originating from the increased cross-linking points and higher cross-linking density (Fig. S7d and Fig. S8a and b).<sup>7</sup> By comparing the pore diameters of PVA/W-AA3-2d and PVA/W-AA3-8d (Fig. S8c and d), it could be concluded that the microstructure of the gels was essentially stabilized after 2 days of induction.

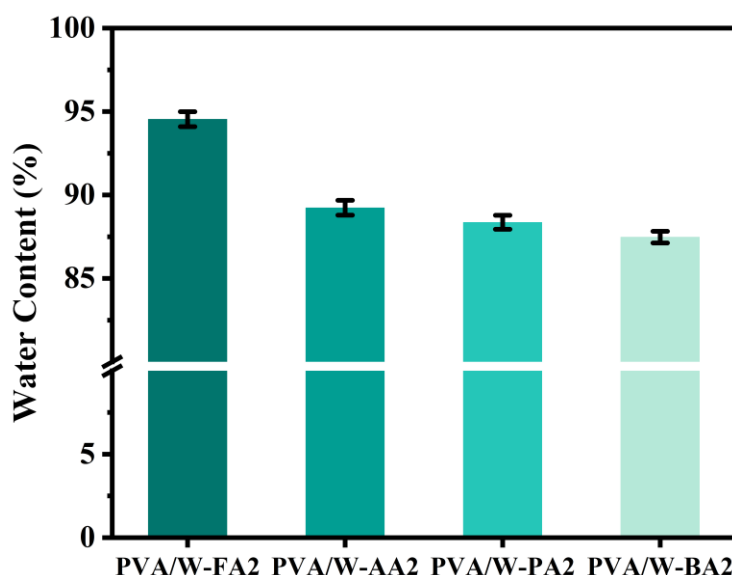


**Fig. S9** The water content of the PVA hydrogels induced by 2 M different monocarboxylic acids.

The water content of the PVA hydrogels was determined by the mass change before and after drying. According to Fig. S9, the water content of the PVA/W-FA2 hydrogels was 94.54%, greatly higher than the theoretical values predicted by feed ratios. The reason for the higher water content is that the PVA chains were loosened and part of them diffused into the external aqueous solution during the solvent exchange process. While the water content of PVA/W-BA2 dropped to 87.48%, proving the formation of a more densely cross-linked structure. This in turn demonstrates that the crosslinking density of PVA physical gels rises along with the lengthening of monocarboxylic acids' alkyl chains.

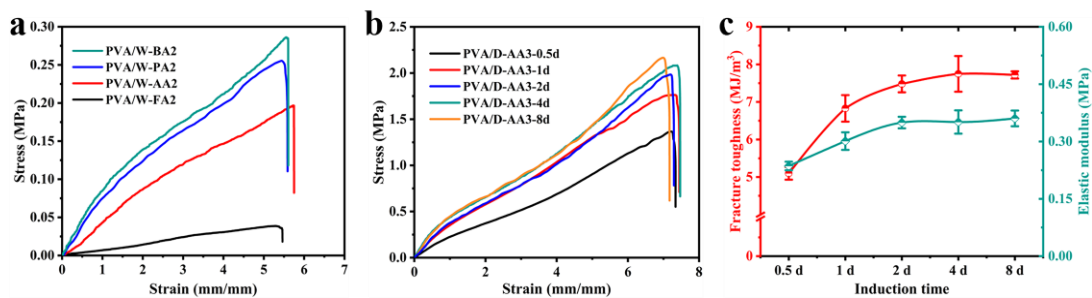


**Fig. S10** (a) Tensile stress-strain curves of the PVA hydrogels induced by 2 M different monocarboxylic acids. (b) Tensile stress-strain curves and (c) elastic modulus and fracture toughness of PVA/D-AA3 gels with different induction times.

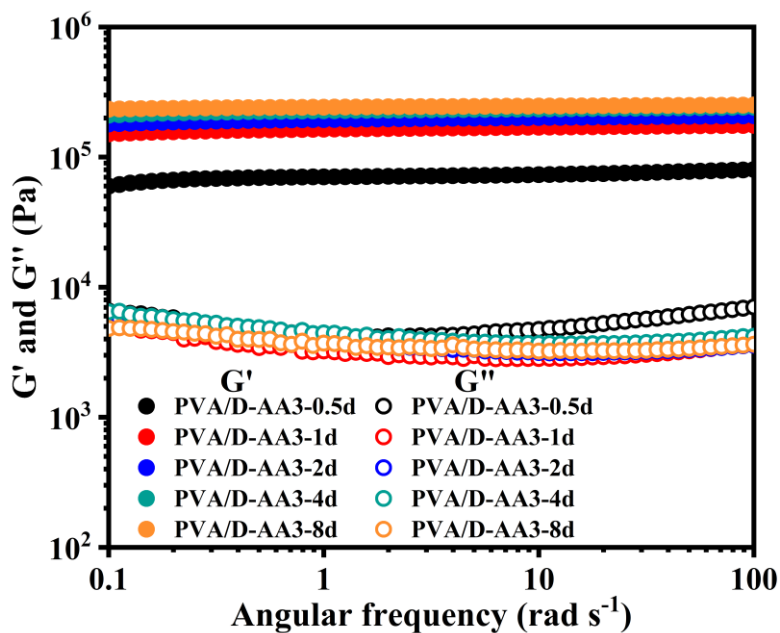


**Fig. S11**  $G'$  and  $G''$  as functions of frequency for PVA/D-AA3 gels with different induction times.

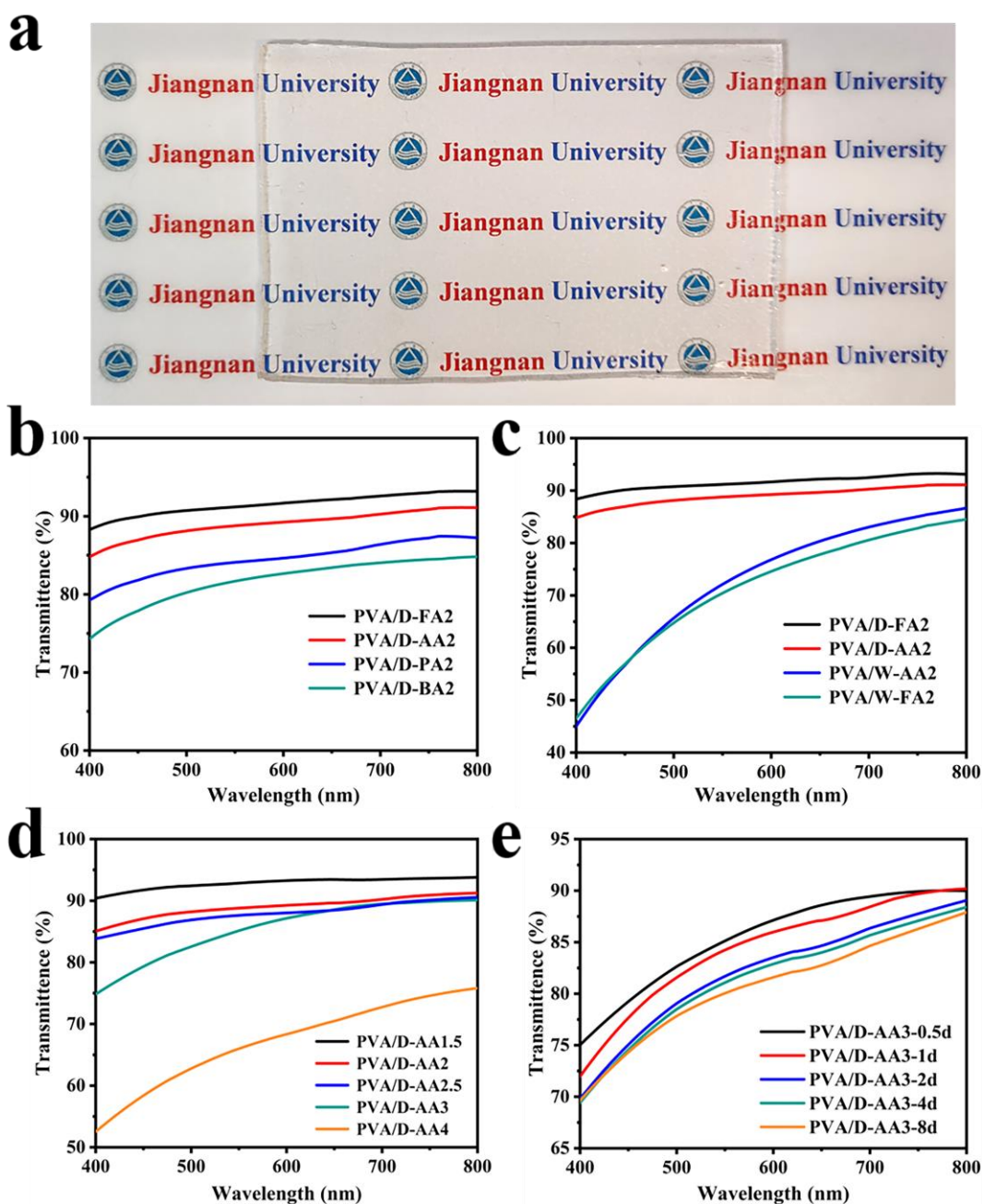


**Fig. S12** (a) Digital image of transparency demonstration. UV-vis spectra of (b) PVA physical gels induced by 2 M different monocarboxylic acids, (c) PVA physical gels and hydrogels induced by 2 M formic acid and acetic acid, (d) PVA/D-AA gels induced by different AA concentrations, and (e) PVA/D-AA3 gels with different induction times.

## REFERENCES

1. S. Lin, J. Liu, X. Liu and X. Zhao, *Proc Natl Acad Sci U S A*, 2019, 116, 10244-10249.
2. N. A. Peppas and E. W. Merrill, *Journal of Applied Polymer Science*, 1976, 20, 1457-1465.
3. S. T. Lin, X. Y. Liu, J. Liu, H. Yuk, H. C. Loh, G. A. Parada, C. Settens, J. Song, A. Masic, G. H. McKinley and X. H. Zhao, *Sci Adv*, 2019, 5, eaau08528.
4. J. Chen, D. Shi, Z. Yang, W. Dong and M. Chen, *Journal of Power Sources*, 2022, 532, 231326.
5. X. N. Zhang, Y. J. Wang, S. Sun, L. Hou, P. Wu, Z. L. Wu and Q. Zheng, *Macromolecules*, 2018, 51, 8136-8146.
6. L. Xu, S. Gao, Q. Guo, C. Wang, Y. Qiao and D. Qiu, *Adv Mater*, 2020, 32, e2004579.
7. F. Wang, Z. Li, J. Guo, L. Liu, H. Fu, J. Yao, I. Krucińska and Z. Draczyński, *ACS Applied Polymer Materials*, 2021, 4, 618-626.